important result was that unlike the ideal link case, the steady-state MSD, EMSE, and MSE are not monotonically increasing functions of step-size when links are noisy. As our simulation results show, there is a good match between theory (our derived expressions) and computer simulations. It must be noted that different learning rules (such as NLMS and RLS) can also be applied in the context of a distributed network with incremental topology. In our future work we will consider the effect of noisy links on the diffusion based distributed adaptive estimation methods.

ACKNOWLEDGMENT

The authors would like to thank Iran Telecommunication Research Center (ITRC) for their financial support of this research.

REFERENCES

[1] C. G. Lopes and A. H. Sayed, "Distributed adaptive incremental strategies: Formulation and performance analysis," in *Proc. IEEE Int. Conf. Acoust., Speech, Signal Process. (ICASSP)*, Toulouse, France, May 2006, vol. 3, pp. 584–587.

[2] C. G. Lopes and A. H. Sayed, "Incremental adaptive strategies over distributed networks," *IEEE Trans. Signal Process.*, vol. 55, no. 8, pp. 4064–4077, Aug. 2007.

[3] A. H. Sayed and C. G. Lopes, "Distributed recursive least-squares strategies over adaptive networks," in *Proc. Asilomar Conf. Signals, Syst., Comput.*, Monterey, CA, Oct. 2006, pp. 233–237.

[4] L. Li, J. A. Chambers, C. G. Lopes, and A. H. Sayed, "Distributed estimation over an adaptive incremental network based on the affine projection algorithm," *IEEE Trans. Signal Process.*, vol. 58, no. 1, pp. 151–164, Jan. 2010.

[5] N. Takahashi and I. Yamada, "Incremental adaptive filtering over distributed networks using parallel projection onto hyperslabs," IEICE Tech. Rep., 2008, vol. 108, pp. 17–22.

[6] C. G. Lopes and A. H. Sayed, "Diffusion least-mean squares over adaptive networks: Formulation and performance analysis," *IEEE Trans. Signal Process.*, vol. 56, no. 7, pp. 3122–3136, Jul. 2008.

[7] F. S. Cattivelli, C. G. Lopes, and A. H. Sayed, "Diffusion recursive least-squares for distributed estimation over adaptive networks," *IEEE Trans. Signal Process.*, vol. 56, no. 5, pp. 1865–1877, May 2008.

[8] A. H. Sayed, *Fundamentals of Adaptive Filtering*. New York: Wiley, 2003.

[9] D. S. Tracy and R. P. Singh, "A new matrix product and its applications in partitioned matrix differentiation," *Statistica Neerlandica*, vol. 26, no. 4, pp. 143–157, 1972.

Filter Bank Property of Multivariate Empirical Mode Decomposition

Naveed ur Rehman and Danilo P. Mandic

***Abstract*—The multivariate empirical mode decomposition (MEMD) algorithm has been recently proposed in order to make empirical mode decomposition (EMD) suitable for processing of multichannel signals. To shed further light on its performance, we analyze the behavior of MEMD in the presence of white Gaussian noise. It is found that, similarly to EMD, MEMD also essentially acts as a dyadic filter bank on each channel of the multivariate input signal. However, unlike EMD, MEMD better aligns the corresponding intrinsic mode functions (IMFs) from different channels across the same frequency range which is crucial for real world applications. A noise-assisted MEMD (N-A MEMD) method is next proposed to help resolve the mode mixing problem in the existing EMD algorithms. Simulations on both synthetic signals and on artifact removal from real world electroencephalogram (EEG) support the analysis.**

***Index Terms*—Filter bank, multivariate empirical mode decomposition (MEMD), mode mixing, noise-assisted MEMD.**

I. INTRODUCTION

The empirical mode decomposition (EMD) algorithm has become an established tool for the decomposition and time-frequency analysis of nonstationary signals [1]. In EMD, the original signal is decomposed as a linear combination of data-driven set of basis functions known as the intrinsic mode functions (IMFs). The IMFs are zero-mean amplitude-frequency modulated (AM-FM) signals, especially designed to ensure that the application of Hilbert transform, known as Hilbert–Huang transform, yields physically meaningful instantaneous frequency estimates of the input signal [2]. Due to the ability of EMD and the Hilbert-Huang transform to process nonstationary data, it has found a number of different real world applications [3], [4].

In recent years, the advances in data acquisition tools have highlighted the need for direct processing of multichannel (multivariate) data; the corresponding multivariate signal processing tools should provide deeper insight into complex and nonstationary real world processes such as wind and inertial body motion data [5]. Multivariate extensions of EMD are a prerequisite for the time frequency analysis of such processes since applying EMD separately on each channel generally yields a different number of misaligned IMFs. On the other hand, recently developed multivariate extensions of EMD, including the complex and bivariate EMD [6], [7], trivariate EMD [8], and multivariate EMD (MEMD) [9] produce the same number of IMFs for all channels, facilitating direct multichannel modelling.

The MEMD algorithm is the first generic extension of standard EMD for multivariate data, and while it has been shown to perform well in deterministic settings involving synthetic sinusoidal signals [9], for its real world applications it is also important to investigate how it behaves in the presence of multichannel white noise. Corresponding analyses for standard EMD revealed that IMFs tend to mimic a filter bank structure, similar to that observed in the case of wavelet decompositions [10], [11]. In the multivariate case, however, a filter bank structure must also ensure the overlapping of the frequency responses of the

Manuscript received June 16, 2010; revised September 23, 2010, January 03, 2011; accepted January 05, 2011. Date of publication January 17, 2011; date of current version April 13, 2011. The associate editor coordinating the review of this manuscript and approving it for publication was Prof. Xiang-Gen Xia.

The authors are with the Department of Electrical and Electronic Engineering, Imperial College London, London SW7 2AZ, U.K. (e-mail: naveed.rehman07@ic.ac.uk; d.mandic@ic.ac.uk).

Digital Object Identifier 10.1109/TSP.2011.2106779

filters associated with the same-index IMFs from multiple channels, as this allows to relate multiple components of a multivariate signal, a crucial requirement in fusion applications [12], [13].

In this work we illustrate that the MEMD does act as a filter bank on white Gaussian noise and show that standard EMD, when applied separately on each channel, fails to effectively align the frequency responses from same-index IMFs of multiple channels. This problem of standard EMD has prompted attempts to generate the so called correlated IMFs from multiple channels, in terms of their frequency contents [14]. MEMD, on the other hand, has been shown to be able to align the frequency subbands from different channels both for single and averaged noise realizations. Based on the improved alignment of frequency subbands in the presence of noise within the MEMD algorithm, a noise-assisted MEMD (N-A MEMD) method is then proposed which tends to enforce quasi-dyadic filter bank structure within the decomposed IMFs and, in turn, helps to accurately align the common oscillatory modes in corresponding IMFs from multiple channels, thus reducing the mode mixing problem across individual channels in multivariate IMFs. This approach is different from the ensemble EMD [15] in which several realizations of white noise are added to the signal in hand, processed via EMD, and then averaged.

II. An Introduction to Multivariate EMD

The multivariate EMD algorithm has been recently proposed in [9] to process a general class of multivariate signals having an arbitrary number of channels.[1] It extends the concept of bivariate EMD [6] and trivariate EMD [8] by processing the input signal directly in a multidimensional domain (n-space), where the signal resides. To achieve that, input signal projections are taken directly along different directions in n-dimensional spaces to calculate the local mean. This step is necessary since calculation of the local mean, a crucial step in EMD algorithm, is difficult to perform due to the lack of formal definition of maxima and minima in higher dimensional domains.

In order to obtain projections of the input signal in n-dimensional spaces, the sampling scheme based on low discrepancy Hammersley sequence was used in [9]. Unlike conventional uniform angular sampling schemes, the sampling scheme based on Hammersley sequence belongs to a class of quasi-Monte Carlo methods, and provides relatively more uniform sampling in higher dimensional spaces [16]. Once the projections along different directions in multidimensional spaces are obtained, their extrema are interpolated via cubic spline interpolation to obtain multiple signal envelopes; these envelopes are then averaged to obtain the local mean of a multivariate signal.

Algorithm 1: Multivariate Extension of EMD

1: Generate the pointset based on the Hammersley sequence for sampling on an $(\mathrm{n}-1)$-sphere [9].
2: Calculate a projection, denoted by $p^{\theta_k}(t)\}_{t=1}^{T}$, of the input signal $\{\mathbf{v}(t)\}_{t=1}^{T}$ along the direction vector $\mathbf{x}^{\theta_k}$, for all k (the whole set of direction vectors), giving $p^{\theta_k}(t)\}_{k=1}^{K}$ as the set of projections.
3: Find the time instants $\{t_i^{\theta_k}\}_{k=1}^{K}$ corresponding to the maxima of the set of projected signals $p^{\theta_k}(t)\}_{k=1}^{K}$.
4: Interpolate $[t_i^{\theta_k}, \mathbf{v}(t_i^{\theta_k})]$, for all values of k, to obtain multivariate envelope curves $\mathbf{e}^{\theta_k}(t)\}_{k=1}^{K}$.
5: For a set of K direction vectors, calculate the mean $\mathbf{m}(t)$ of the envelope curves as

$$\mathbf{m}(t) = \frac{1}{K}\sum_{k=1}^{K}\mathbf{e}^{\theta_k}(t). \tag{1}$$

6: Extract the "detail" $d(t)$ using $d(t) = x(t) - m(t)$. If the "detail" $d(t)$ fulfills the stoppage criterion for a multivariate IMF, apply the above procedure to $x(t) - d(t)$, otherwise apply it to $d(t)$.

Consider a sequence of N-dimensional vectors $\{\mathbf{v}(t)\}_{t=1}^{T} = \{v_1(t), v_2(t), \ldots, v_N(t)\}$ representing a multivariate signal with N components, and $\mathbf{x}^{\theta_k} = \{x_1^k, x_2^k, \ldots, x_N^k\}$ denoting a set of direction vectors along the directions given by angles $\theta^k = \{\theta_1^k, \theta_2^k, \ldots, \theta_{(N-1)}^k\}$ on an $(\mathrm{n}-1)$-sphere. Then the extraction of the first IMF from the proposed multivariate extension of EMD is summarized in Algorithm 1.

Once the first IMF is extracted, it is subtracted from the input signal and the same process (Algorithm 1) is applied to the resulting signal yielding the second IMF and so on; the process is repeated until all the IMFs are extracted and only a residue is left; in the multivariate case, the residue corresponds to a signal whose projections do not contain enough extrema to form a meaningful multivariate envelope. The sifting process for a multivariate IMF can be stopped when all the projected signals fulfill any of the stoppage criteria adopted in standard EMD. One popular stopping criterion used in EMD stops the sifting when the number of extrema and the zero crossings differ at most by one for S consecutive iterations of the sifting algorithm[2] [17]. Another commonly used criterion introduces an evaluation function based on the envelope amplitude, defined as: $a(t) = (1/K)\sum_{k=1}^{K}|e^{\theta^k}(t) - m(t)|$. The sifting process is continued until the value of the evaluation function, defined as $f(t) = |(m(t)/a(t))|$ where $m(t)$ is the local mean signal, is less than or equal to some predefined thresholds σ [18]. Both these criteria have been used in the simulations presented in this work.

III. Filter Bank Property of MEMD

Filter banks represent a collection of bandpass filters designed to isolate different frequency bands in the input signal. It was shown in [10] and [11] that the IMFs obtained from standard EMD algorithm provide frequency responses similar to that of a dyadic filter bank. In this section, we set out to investigate whether this filter bank structure is preserved by MEMD for multichannel input signals.

It is worth emphasizing that the idea of a filter bank for multivariate inputs, in a strict sense, is still ambiguous since the concept of frequency is not clearly defined for multivariate signals. However, even if we consider the frequency response for the individual channels of a multivariate signal, the filter bank structure imposes an additional constraint on the frequency output of each multivariate IMF—*the overlapping of the filter bands associated with the corresponding (same-index) IMFs from multiple channels*. This is vital for the IMFs obtained from MEMD to be physically meaningful; any mismatch in the frequency contents of the corresponding multichannel IMFs would render their matching or subsequent fusion applications meaningless.

The frequency response and the corresponding filter bank property of MEMD are first illustrated by applying MEMD on a single realization of an eight-channel white Gaussian noise; the power spectra of its resulting first fine IMFs are plotted in the top of Fig. 1. Next, the same eight noise channels were separately processed via standard EMD and the estimated power spectra of its IMFs are shown in the bottom of Fig. 1. It can be seen that the overlapping of frequency bands of same-index IMFs associated with different channels is much more prominent in the case of MEMD as compared with standard EMD. The alignment of IMF based frequency bands for single noise realization, in case of MEMD, results in the stabilization of the shape of individual spectra and allows for the estimation of these spectra using fewer noise

[1]The Matlab code for multivariate EMD along with some synthetic and real world multivariate signals are available from http://www.commsp.ee.ic.ac.uk/~mandic/research/emd.htm.

[2]Caution must be exercised while using this criterion for multivariate cases as it has been found to be computationally very expensive for long signals.

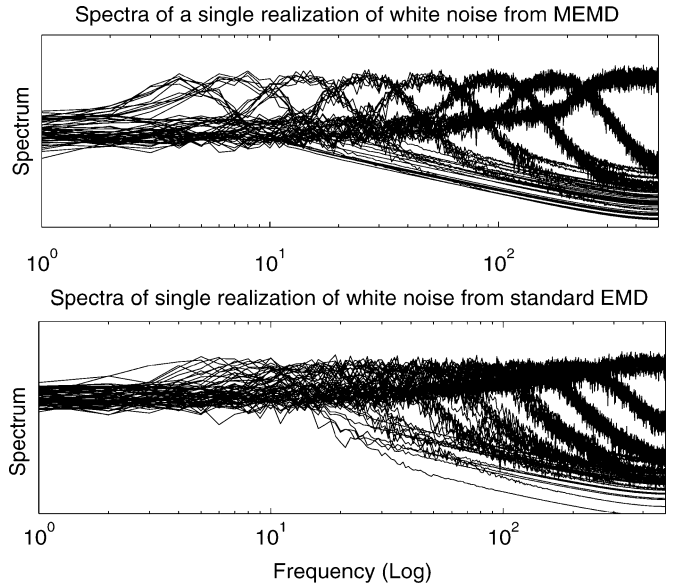

Fig. 1. Spectra of IMFs (IMF1-IMF9) obtained for a single realization of an eight-channel white Gaussian noise via MEMD (top) and the standard EMD (bottom). Overlapping of the frequency bands corresponding to the same-index IMFs is more prominent in the case of MEMD based filters.

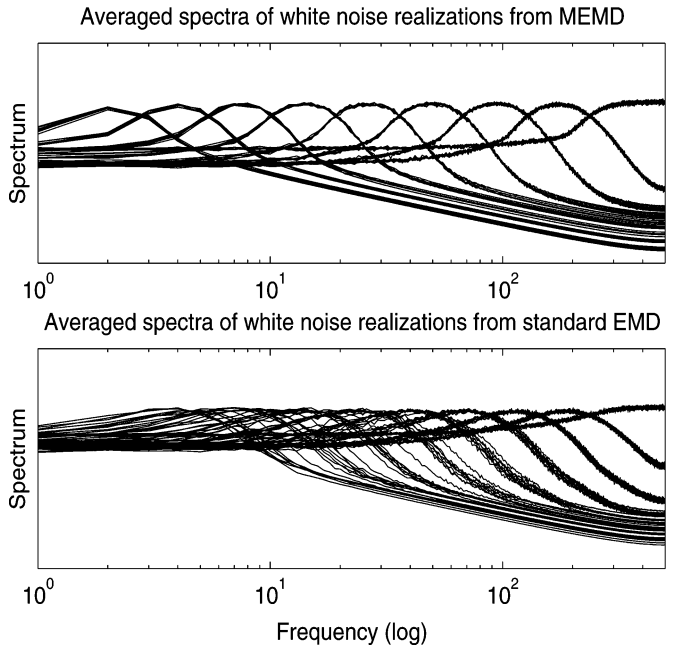

Fig. 2. Averaged spectra of IMFs (IMF1-IMF9) obtained for a $N = 500$ realizations of eight-channel white Gaussian noise via MEMD (top) and the standard EMD (bottom). Overlapping of the frequency bands corresponding to the same-index IMFs is improved in both cases but the MEMD bands clearly show much better alignment.

realizations as illustrated in Fig. 2. In simulations, we used $N = 500$ noise realizations each of length $T = 1000$ which were then ensemble averaged to yield an averaged power spectra; the stopping criteria used is given in [17], with the value of $S = 5$. It is evident from the Fig. 2 that for a given number of noise realizations N, standard EMD failed to properly align the bandpass filters associated with the corresponding IMFs for different noise channels. Although this alignment is expected to become better with an increase in the number of noise realizations, MEMD based spectra achieved much better results with same number of ensembles.

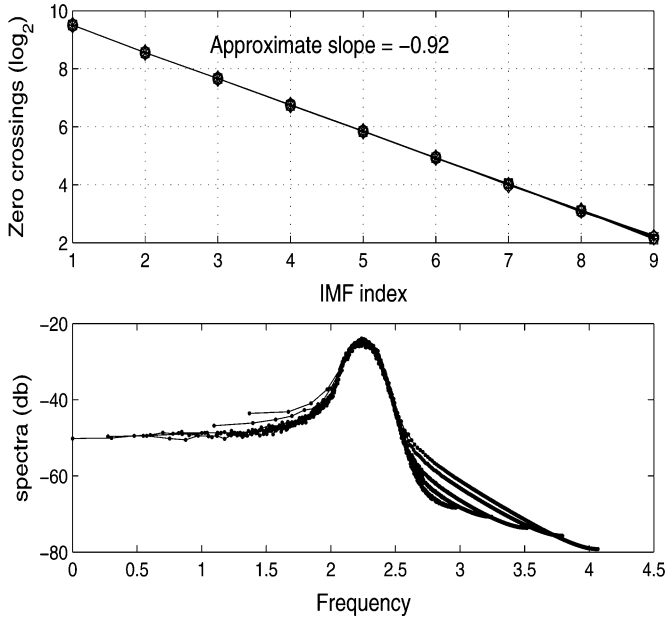

Fig. 3. MEMD as a dyadic filter bank. Top: Average number of base-2 logarithm of zero crossings plotted versus the IMF index for all eight channels. The slope of -0.92 indicates similarity to a dyadic filter (with an ideal slope -1). Bottom: Fourier spectra of IMFs from MEMD with IMF3-IMF9 shifted so as to overlap with the spectrum associated with IMF2.

Since the number of zero crossings in an IMF is directly related to the number of intrinsic oscillations, as a rough indicator of the frequency content within the IMF, this makes it possible to analyze the nature of MEMD as a filter bank with respect to the IMF index. For standard EMD, it was shown in [10] and [11] that the IMFs followed the structure of a dyadic filter with the linear (slope close to -1) relationship between the base-2 logarithm of number of zero crossings and the IMF index. Fig. 3 (top) shows the results obtained by applying MEMD on eight-channel white noise, plotted using the base-2 logarithm of zero crossings of IMFs of individual channels against the IMF index. It revealed similar results to those obtained from standard EMD, with the slope of approximately -0.92 for all the eight channels individually, indicating a quasi-dyadic filter bank nature of MEMD for white noise. The stopping criteria used was the S-stopping criterion [17], with the value of $S = 5$. The filter bank structure may be slightly affected by the number of sifting iterations employed, and possibly by the type of stopping criteria used, as mentioned briefly in [19], for a single-channel EMD.

Another important property of standard EMD based filter bank is the self-similarity of its constituent bandpass filters [10]. To illustrate that the IMFs of individual channels obtained from MEMD also exhibit this self-similar behavior, let $H_n(f)$ denote the frequency response of the nth IMF. Then due to the similarity between different IMF based bandpass filters, the frequency response of kth IMF can be described by

$$H_k(f) = H_n(f)(\gamma^{k-n} f) \tag{2}$$

where $k > n \geq 2$. Parameter γ can be calculated from the slope of the straight line.[3] between the number of zero crossings and the IMF index; for a fully dyadic filter bank, its value is 2. Using the normalized (2), the spectra of all the IMFs obtained from MEMD collapsed to a single curve as shown in Fig. 3 (bottom).

[3]The empirical relationship between the center frequency and the bandpass filter index (IMF index) can be approximated by $\log_2 F_x = mx + c$, where F_x denotes the estimated center frequency corresponding to the IMF index x and c represents the y-intercept of the straight line and is dependent on the total number of IMFs obtained [20].

This shows that the IMFs obtained by MEMD follow the quasi-dyadic filter bank structure similar to the IMFs from standard EMD both for single channel and for multiple channels, facilitating applications based on vector sensors and in time-frequency data fusion.

IV. Noise-Assisted MEMD

We now introduce a noise-assisted MEMD (N-A MEMD) method which makes use of the quasi-dyadic filter bank properties of MEMD on white noise, and show that it is capable of significantly reducing the mode mixing problem[4] for classes of signals where the quasi-dyadic filter bank structure proves useful.

Embarking upon the quasi-dyadic filter bank structure of standard EMD for broadband noise, Wu *et al.* proposed the ensemble EMD method in which multiple realizations of white noise are added to the input signal before being decomposed via EMD. This helps to establish a uniformly distributed reference scale which, in turn, results in corresponding IMFs exhibiting a quasi-dyadic filter bank structure. Finally, their ensemble mean is taken which cancels the noise effect within the IMFs.

In the same spirit, to explore the benefits of quasi-dyadic filter bank structure of MEMD on white noise, we propose to add extra channels containing multivariate independent white noise to the original multivariate signal, and then process such a composite signal via MEMD. The IMF channels corresponding to white noise are then discarded yielding a set of IMFs associated with only the original input signal. Since the added noise channels occupy a broad range in the frequency spectrum, MEMD aligns its IMFs based on the quasi-dyadic filter bank, with each component carrying a frequency subband of the original signal. In doing so, IMFs corresponding to the original input signal also align themselves according to the structure of a quasi-dyadic filter bank (see Fig. 2); this, in turn, helps to reduce the mode mixing problem within the extracted IMFs. The details of the NA-EMD method are outlined in Algorithm 2.

Algorithm 2: Noise-Assisted MEMD

1: Create an uncorrelated Gaussian white noise time-series (m-channel) of the same length as that of the input;
2: Add the noise channels (m-channel) created in Step 1 to the input multivariate (n-channel) signal, obtaining an $(n + m)$-channel signal;
3: Process the resulting $(n + m)$-channel multivariate signal using the MEMD algorithm listed in Algorithm 1, to obtain multivariate IMFs;
4: From the resulting $(n+m)$-variate IMFs, discard the m channels corresponding to the noise, giving a set of n-channel IMFs corresponding to the original signal.

However, it should be mentioned that the so-called noise-assisted methods (both ensemble EMD and N-A MEMD) for reducing the mode mixing problem are expected to be most useful for signals in which the dyadic filter bank decomposition is relevant. For instance, if the desired signal resides in multiple dyadic subbands, then choosing these noise-assisted methods for decomposition may even "spread" the desired signal across multiple IMFs, resulting in unwanted mode mixing.

To illustrate the operation of N-A MEMD further, consider a synthetic signal consisting of a combination of three different tones; two low-frequency tones were added together along with a high-frequency sinusoid which was only added between the time index 5000 and 8500. The resulting signal is shown in the top of Fig. 4. Also shown in Fig. 4 are the IMFs obtained from applying standard EMD to the signal; mode mixing is evident since IMF1 contains multiple modes. Similarly, mode mixing can also be seen in IMF2 and IMF3. We next processed the same signal using the proposed N-A MEMD method with two extra noise channels $(m = 2)$. The IMFs from the resulting trivariate signal are shown in Fig. 5. Observe that the IMFs corresponding to the first channel are now free of mode mixing, as all the tones are decomposed as separate IMFs (IMF6, IMF7, and IMF8, respectively).

In the proposed N-A MEMD method, the number of noise channels m and the amplitude of noise channels must be chosen so that the desired dyadic filter bank structure is enforced. In our experiments with the selected synthetic signals, as expected, we found a reduction in the

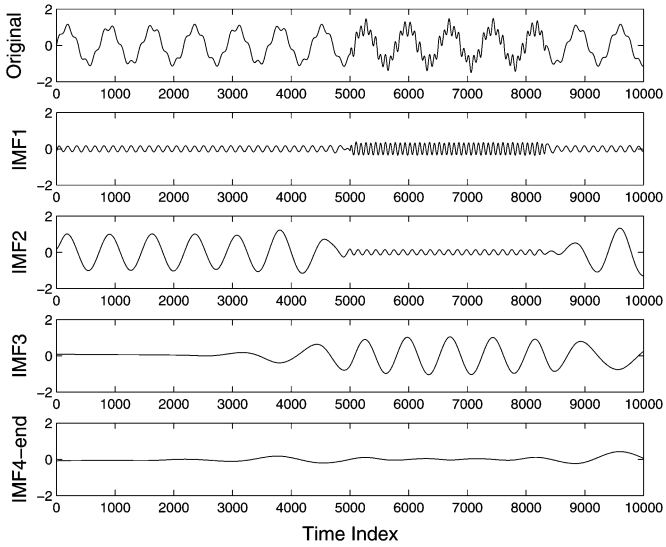

Fig. 4. IMFs of a synthetic signal obtained by applying standard EMD. Mode mixing is evident in IMF1, IMF2 and IMF3 where either multiple modes are present (IMF1 and IMF2) or a single mode is "leaked" into two IMFs (IMF2 and IMF3).

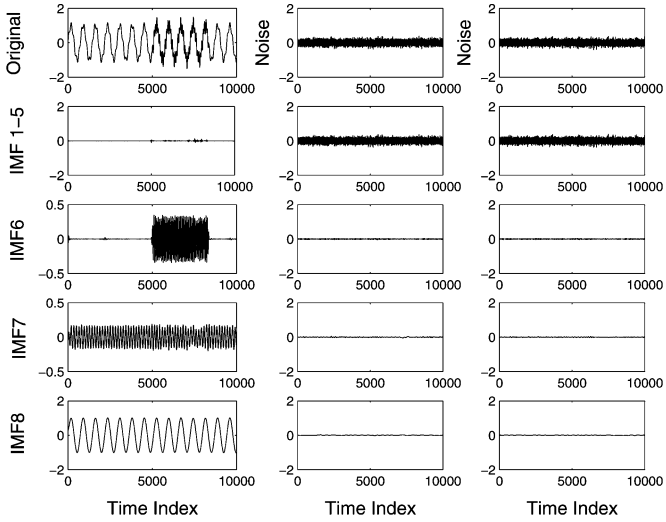

Fig. 5. IMFs of synthetic signal obtained by applying the N-A MEMD (left hand column); the IMFs of the two noise channels shown in the middle and right hand column. Mode mixing observed in IMFs from standard EMD is significantly reduced with IMF6, IMF7, and IMF8 containing the three original tones (see text for more detail).

[4]Mode mixing is characterized by a single IMF containing multiple oscillatory modes and/or a single mode residing in multiple IMFs which may compromise the physical meaning of IMFs and practical applications in certain cases. This problem may be caused by the intermittency of the input signal and/or variation of instantaneous amplitude and frequency of the modes and affects both the standard and multivariate EMD.

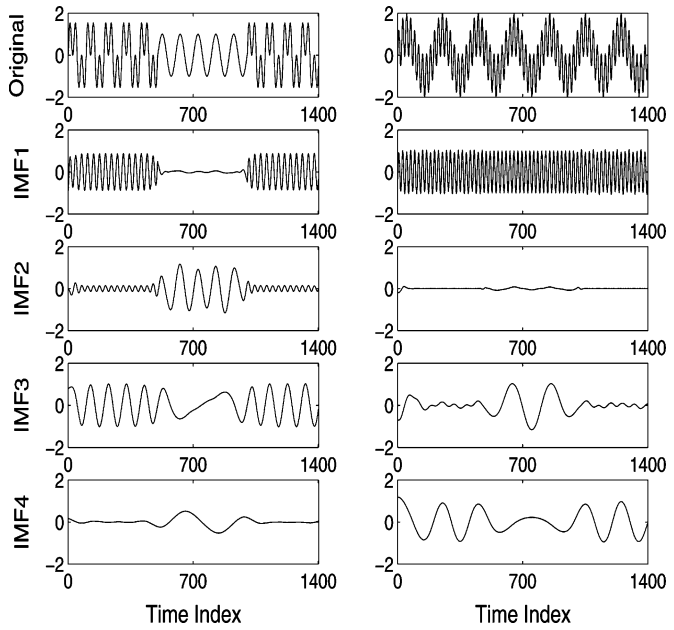

Fig. 6. Decomposition of a synthetic bivariate tone signal using the bivariate EMD. Mode mixing and mode misalignment are evident across all but the IMF1. Simulations with different parameters for the stopping criterion yielded similar results.

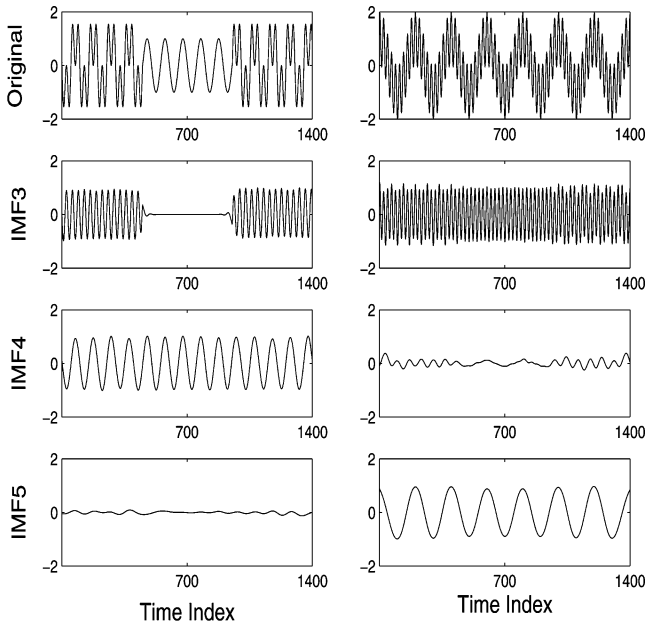

Fig. 7. Decomposition of a synthetic bivariate tone signal via noise-assisted MEMD for $m = 2$. Both the problems of mode mixing and mode misalignment are clearly reduced. Again, the obtained results were generally found robust to variations in the parameters.

amount of mode mixing with an increase in both m and the amplitude of the noise. However, it also caused some "leakage" from noisy channels into the input channel which resulted in slight disturbance in the desired signal, implying a trade-off in practice, whose dependence on MEMD parameters still needs to be further explored. The amount of "leakage" was found to be small though and should be negligible in most practical scenarios. In cases where it is significant, similarly to approach used in ensemble EMD [15], we may consider adding multiple realizations of white noise to the input signal channel and average them out to reduce the "leakage" effect; this correction would, however, result in increased computational complexity.

We next performed simulations on a synthetically generated combination of tones[5] to show that the introduction of noise reduces the "mode-misalignment" in multivariate extensions of EMD. As stated earlier, mode alignment refers to the generation of similar frequency modes across same-index IMFs in multiple channels, and is one of the characteristics of multivariate extensions of EMD [9]. However, in addition to the mode mixing within IMFs of a single channel, as illustrated in Fig. 4, the intermittence in the input data also results in mode-mixing within the same-indexed IMFs of multiple channels (mode misalignment). This is illustrated in Fig. 6, which shows the decomposition of a synthetically generated bivariate tone signal via bivariate extension of EMD [6]. While the highest frequency mode was correctly decomposed as IMF1, both mode mixing in a single channel and mode misalignment across multiple channels are evident in the remaining IMFs; a single frequency mode was shared in both IMF2 and IMF3 in the first channel and also in IMF3 and IMF4 in the second channel (mode mixing). Also, different frequency modes can be seen across different channels in IMF3 (mode misalignment).

Fig. 7 shows the decomposition of the same bivariate signal obtained by the proposed N-A MEMD method, with two extra channels of white noise $(m = 2)$. For convenience, the channels corresponding to the white noise have not been plotted. It can be seen that, in this case, both mode mixing and mode misalignment are significantly reduced, with each IMF carrying only a single frequency mode, and no instance of different modes across same-index IMFs of different channels. This was expected because the quasi-dyadic structure enforced by the addition of noisy channels in N-A MEMD resulted in the alignment of frequency subbands from different channels of the multivariate signal, in turn, resulting in "aligned" IMFs in terms of their frequency contents.

[5]The complex part is a combination of two tones (0.5 and 3 KHz), whereas the real part consists of a combination of a tone of 1 KHz, and a tone of 3 KHz, added only at the beginning and the end of the signal.

V. Real World EEG Signal Processing via MEMD

In order to demonstrate the advantages of MEMD in multichannel signal processing and its ability to align common frequency modes in same-index IMFs, we applied the proposed method to the real world electroencephalography (EEG) signals with an aim to separate the brain electrical activity from unwanted artefacts, such as the electrooculogram (EOG) and electromyogram (EMG). Data used in these simulations were collected from 4 EEG channels $(Fp1, Fp2, C3, C4)$, and subjects were asked to move their eyes during the data collection, resulting in the ocular interference in the recorded EEG signal. The four channels were then processed by MEMD.

Owing to the property of MEMD to align IMF frequency subbands from different channels, the decomposed EEG data was aligned in such a way that the high-frequency neurophysiological signals were contained in the lower-index IMFs, while low-frequency electrophysiological signals (EMG and EOG) were present in the higher-index IMFs. A simple threshold on the IMF index was then used to separate non-EEG related interference from the underlying brain activity. The EOG and clean EEG signal estimated in this way are shown in the middle and right hand column of Fig. 8, with the original contaminated EEG signals shown in the left hand column. It is important to note that such separation is difficult to achieve by applying univariate EMD to all the channels separately, as this would result in spectrally uncorrelated components, as evidenced in the bottom diagram of Fig. 2. For this purpose, a complex clustering technique was used in the frequency

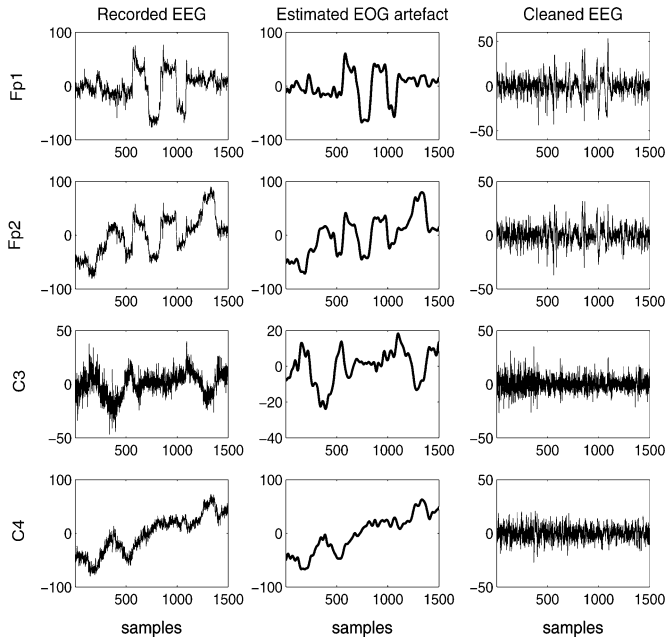

Fig. 8. Artefact removal from four EEG channels ($Fp1, Fp2, C3$ and $C4$) using the MEMD algorithm. The estimated eye muscle activity (artefact) has been shown in the middle column, whereas the conditioned EEG signal is presented in the right hand column.

domain (Hilbert–Huang spectrum) in order to identify spatially correlated modes from univariate EMD decompositions [21]. However, as EMD was applied channelwise, high-frequency components were still present in the estimated EOG signal.[6]

VI. Conclusion

We have shown that the multivariate empirical mode decomposition (MEMD) algorithm follows a filter bank structure (channelwise) for a multivariate white noise input. It has also been shown that MEMD aligns similar modes present across multiple channels in same-index IMFs, which is difficult to obtain by applying standard EMD channelwise. Furthermore, by using the property of MEMD to behave as a filter bank in the presence of white noise, we have proposed a noise-assisted MEMD (N-A MEMD) algorithm, whereby by introducing extra channels of multivariate noise, the effects of mode mixing and mode misalignment in multivariate IMFs have been reduced. Unlike ensemble EMD, where several realizations of white noise are directly added to the signal and then multiple instances of EMD are run, the framework of MEMD allows adding white noise in extra channels and hence only a single application of MEMD is sufficient. The analysis is supported by simulations on both synthetic and real world multivariate data.

References

[1] N. E. Huang, Z. Shen, S. Long, M. Wu, H. Shih, Q. Zheng, N. Yen, C. Tung, and H. Liu, "The empirical mode decomposition and Hilbert spectrum for non-linear and non-stationary time series analysis," in *Proc. Roy. Soc. A*, 1998, vol. 454, pp. 903–995.

[2] *Hilbert-Huang Transform and Its Applications*, N. E. Huang and S. S. P. Shen, Eds. Singapore: World Scientific, 2005.

[6]The example presented here aims to highlight the advantages of the mode alignment property of MEMD in multichannel signal processing; for more advanced EMD based denoising techniques, refer to [20].

[3] I. M. Janosi and R. Muller, "Empirical mode decomposition and correlation properties of long daily ozone records," *Phys. Rev. E*, vol. 71, no. 056126, 2005.

[4] N. E. Huang and Z. Wu, "A review on Hilbert-Huang transform: Method and its applications to geophysical studies," *Rev. Geophys.*, vol. 46, no. RG2006, 2008.

[5] D. P. Mandic and V. S. L. Goh, *Complex Valued Non-Linear Adaptive Filters: Noncircularity, Widely Linear Neural Models*. New York: Wiley, 2009.

[6] G. Rilling, P. Flandrin, P. Goncalves, and J. M. Lilly, "Bivariate empirical mode decomposition," *IEEE Signal Process. Lett.*, vol. 14, pp. 936–939, 2007.

[7] T. Tanaka and D. P. Mandic, "Complex empirical mode decomposition," *IEEE Signal Process. Lett.*, vol. 14, no. 2, pp. 101–104, 2006.

[8] N. Rehman and D. P. Mandic, "Empirical mode decomposition for trivariate signals," *IEEE Trans. Signal Process.*, vol. 58, no. 3, pp. 1059–1068, Mar. 2010.

[9] N. Rehman and D. P. Mandic, "Multivariate empirical mode decomposition," in *Proc. Roy. Soc. A*, 2010, vol. 466, pp. 1291–1302.

[10] P. Flandrin, G. Rilling, and P. Goncalves, "Empirical mode decomposition as a filter bank," *IEEE Signal Process. Lett.*, vol. 11, no. 2, pp. 112–114, 2004.

[11] Z. Wu and N. E. Huang, "A study of the characteristics of white noise using the empirical mode decomposition method," in *Proc. Roy. Soc. A*, 2004, vol. 460A, pp. 1597–1611.

[12] D. Looney and D. P. Mandic, "Multi-scale image fusion using complex extensions of EMD," *IEEE Trans. Signal Process.*, vol. 57, no. 4, pp. 1626–1630, 2009.

[13] *Signal Processing Techniques for Knowledge Extraction and Information Fusion*, D. P. Mandic, Ed. *et al.* New York: Springer, 2008.

[14] T. Rutkowski, D. P. Mandic, A. Cichocki, and A. W. Przybyszewski, "EMD approach to multichannel EEG data—The amplitude and phase components clustering analysis," *J. Circuits, Syst., Comput. (JCSC)*, vol. 19, no. 1, pp. 215–229, 2010.

[15] Z. Wu and N. E. Huang, "Ensemble empirical mode decomposition: A noise-assisted data analysis method," *Adv. Adapt. Data Anal.*, vol. 1, pp. 1–41, 2009.

[16] J. Cui and W. Freeden, "Equidistribution on the sphere," *SIAM J. Sci. Comput.*, vol. 18, no. 2, pp. 595–609, 1997.

[17] N. E. Huang, M. Wu, S. Long, S. Shen, W. Qu, P. Gloersen, and K. Fan, "A confidence limit for the empirical mode decomposition and Hilbert spectral analysis," in *Proc. Roy. Soc. Lond. A*, 2003, vol. 459, pp. 2317–2345.

[18] G. Rilling, P. Flandrin, and P. Gonalves, "On empirical mode decomposition and its algorithms," in *Proc. IEEE-EURASIP Workshop Nonlinear Signal Image Process. (NSIP)*, 2003, Grado (I).

[19] Y. Kopsinis and S. McLaughlin, "Development of EMD-based denoising methods inspired by wavelet threshholding," *IEEE Trans. Signal Process.*, vol. 57, no. 4, pp. 1351–1362, Apr. 2009.

[20] P. Flandrin, P. Goncalves, and G. Rilling, "EMD equivalent filter banks, from interpretations to applications," in *Hilbert-Huang Transform and Its Applications*. Singapore: World Scientific, 2005, pp. 57–74.

[21] T. M. Rutkowski, A. Cichocki, T. Tanaka, D. P. Mandic, J. Cao, and A. L. Ralescu, "Multichannel spectral pattern separation—An EEG processing application," in *Proc. IEEE Int. Conf. Acoust., Speech, Signal Process.*, 2009, pp. 373–376.